High-resolution dielectric spectroscopy and electric-field dependence of carbon allotropes including multiwall and single-wall nanotubes

Rajratan Basu and Germano S. Iannacchione[a)]
Department of Physics, Worcester Polytechnic Institute, Worcester, Massachusetts 01609, USA

(Received 30 November 2007; accepted 21 January 2008; published online 7 February 2008)

High-resolution isothermal dielectric spectroscopy is reported as a function of frequency up to 10^5 Hz and electric field E_{rot} on four carbon allotropes; amorphous glass, diamond, multiwall nanotubes (MWNTs), and single-wall nanotubes (SWNTs). The diamond spectra are featureless while the glass, MWNT, and SWNT samples exhibit two modes. A common low-frequency mode, likely due to surface space charges, is observed at ~16 Hz that decreases in dispersion strength and increases in frequency linearly with increasing E_{rot}. A higher-frequency mode, different for each sample, is also observed having a dispersion strength and frequency independent of E_{rot}. © *2008 American Institute of Physics*. [DOI: 10.1063/1.2841826]

Carbon is an element of great technical importance and interest to industry and science. Pure carbon occurs as several different allotropes, or structures, that differ only in the arrangement of the atoms. Since their discovery in 1991,[1] carbon nanotubes (CNTs) have been studied extensively for their unique electrical, thermal, mechanical, and magnetic properties.[2–12] Recently, composites of CNT within ceramic metals such as alumina[13] or polymers such as polycarbonate[14] have been explored in order to improve their dielectric properties.

The complex dielectric constant $\varepsilon^*=\varepsilon'-i\varepsilon''$ of a material is determined by the molecular polarizability and structural arrangement. This is essentially a measure of a charge-free sample's response to an applied electric field. The real part of the dielectric constant $\varepsilon'(\omega)$ is associated with the storage of the electric field energy while the imaginary part $\varepsilon''(\omega)$ corresponds to the dissipation of energy through a relaxation process. Typically, relaxations below 100 Hz are due to normal conduction while those between 100 and 10^5 Hz are associated reorientation of permanent and/or induced molecular dipoles in the material. Molecular interactions play an important role in such relaxation processes. Changes in the structural arrangement of the molecules can also induce large changes in the dielectric spectra, leading to its use in the study of phase transitions.[15] Dielectric spectroscopy can provide detailed information on dynamic modes, such as segmental mobility of the molecules or vibrational modes of a solid.

In this paper, we use an ac-capacitance bridge technique[16] to measure the isothermal dielectric spectra from 1 to 10^5 Hz of four different carbon structures; amorphous glass, crystalline diamond, single-wall nanotubes (SWNTs), and multiwall nanotubes (MWNTs). In addition, the electric field dependence was probed by increasing the magnitude of the ac-electric field used in the capacitive measurement. The real and imaginary parts of the complex dielectric constant are determined from the in-phase and $(\pi/2)$ out-of-phase off-balance signal of the bridge. Because of the experimental arrangement, the actual magnitude of E_{rot} across the sample is not known (only the driving voltage was controlled). However, the factor by which E_{rot} increases is known if measured in units of that produced by the lowest voltage (denoted as E_{rot}^0 for applied 1 V), this normalized field is labeled $e_R=E_{rot}/E_{rot}^0$. The capacitive cell consists of a parallel-plate configuration, 1 cm across and 100 μm thick using a Kapton spacer, housed in a temperature controlled bath. Comparison between the empty and sample filled capacitors allows for an absolute measurement of $\varepsilon^*(\omega,e_R)$.

All carbon samples were of powder form. The glass sample consisted of spherical particles of 2–12 μm in diameter and 99.95% pure. The diamond sample was of natural monocrystalline form approximately 1 μm in size and 99.9% pure. These powders were obtained from Aldrich and used after degassing under vacuum at 100 °C. The MWNT sample contains nanotubes of 10–100 nm in diameter and 1–5 μm in length. The SWNT sample contains nanotubes ~1.3 nm in diameter and 0.5–50 μm in length. Both carbon nanotube samples were received from Sinha and used without further processing.

The same amount by mass of each sample was loaded into the capacitor cell. The orientation of CNTs was completely random as was the distribution of the diamond and amorphous powders, thus, only the average dielectric constant was determined. For consistency, the same thermal history was applied to each sample and all measurements reported here were performed at a fixed temperature of 328 K (55 °C) with a stability of ±0.005 °C. Temperature dependent experiments on all samples from 300 to 350 K reveal essentially identical spectra indicating that, at least, volatile impurities, which may have been adsorbed onto the carbon, do not play a significant role.

The dielectric spectra for the diamond powder sample reveal no features over the entire frequency range studied. An increase in ε' and ε'' is seen below 10 Hz and is attributed to the onset of normal static conduction. Given the static nature observed, a detailed electric field dependence study was not carried out on diamond. For powders of glass, MWNT, and SWNT carbon, the dielectric spectra exhibit two prominent features, clearly seen in Figs. 1–3, respectively. A low-frequency feature (denoted as mode 1), between 16 and 80 Hz and common to these three samples, is observed to decrease in dispersion strength (peak magnitude of ε'') and shifts to higher frequencies linearly with increasing e_R. The characteristics of mode 1 suggests that it is re-

a)Electronic mail: gsiannac@wpi.edu

 © 2008 American Institute of Physics
Downloaded 19 May 2008 to 130.215.36.230. Redistribution subject to AIP license or copyright; see http://apl.aip.org/apl/copyright.jsp

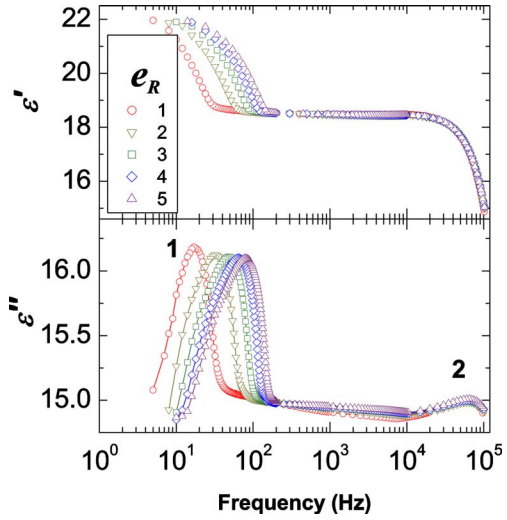

FIG. 1. (Color online) The electric field intensity dependence of $\varepsilon'(\omega)$ and $\varepsilon''(\omega)$ for the amorphous carbon sample. Upper panel legend lists the applied field factor e_R. In $\varepsilon''(\omega)$, the low-frequency mode is denoted by 1 while the high-frequency mode is denoted by 2.

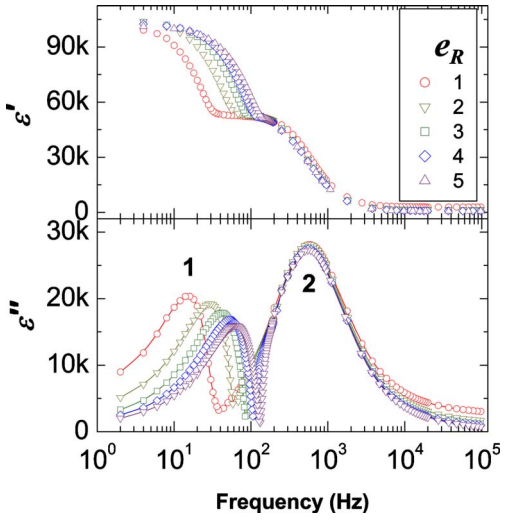

FIG. 3. (Color online) The electric field intensity dependence of $\varepsilon'(\omega)$ and $\varepsilon''(\omega)$ for the SWNT sample (in units of 1000). Upper panel legend lists the applied field factor e_R. For $\varepsilon''(\omega)$, the low-frequency mode is denoted by 1 and the high-frequency mode is denoted by 2.

lated to space charge polarization, which may involve several mechanisms of charge built up at the particle surface or electrode-sample interface.[17] Table I gives the result of a linear regression of the mode-1 peak frequency as a function of e_R.

A higher-frequency feature (mode 2) is observed for the glass, MWNT, and SWNT samples whose peak frequencies occur at 63, 1.9, and 0.6 KHz, respectively, independent of e_R. In addition, the magnitude of the mode-2 dispersion peak is also independent of e_R and exhibits markedly different appearance for the glass than for either of the nanotube samples. The behavior of this mode is consistent with orientational polarization of molecular permanent and/or induced dipoles in the different samples.

To further illuminate the nature of the observed spectra, a "Cole–Cole" construction[18,19] is performed for the glass, MWNT, and SWNT samples. In making this construction, the complex dielectric constant is written as, $\varepsilon^* = \varepsilon_\infty + \Delta\varepsilon(1+i\omega\tau)^{-\beta} - \alpha i(\sigma_0/\omega\varepsilon_{\text{vac}})$ where $\Delta\varepsilon = \varepsilon_\infty - \varepsilon_0$ is the dielectric strength. Here, ε_∞ is the dielectric constant of the material at infinite frequency, ε_0 is the static dielectric constant, ω is the frequency, τ is the relaxation time constant, and β is the fitting factor (where normally $0<\beta<1$). The last term describes electronic conduction where α is the conduction factor, σ_0 is the static conductivity, and ε_{vac} is the vacuum permittivity. For $\alpha=0$, i.e., negligible conduction, this relation yields the Cole–Davidson form[20] while setting $\beta=\alpha=1$ results in the Debye dispersion relation with a static conductivity.[21,22] For $\beta=1$ and $\alpha=0$, a plot of the same scaled units of $\varepsilon''(\omega)$ versus $\varepsilon'(\omega)$ (a Cole–Cole plot) would reveal a semicircle for a single well-defined relaxation process whose diameter is $\Delta\varepsilon$. However, dc conductivity, resulting in a divergence of $\varepsilon''(\omega\to 0)$ or a distribution of relaxation times ($\beta<1$), will lead to distortions of the semicircle.[23,24] Figure 4 shows a Cole–Cole plot for the glass, MWNT, and SWNT carbon samples at the same e_R revealing two well-separated features for each sample. Clearly, Fig. 4 indicates that mode 2 for the glass sample does not represent a typical relaxation process while mode 2 for the MWNT and SWNT samples are similar to each other, though at different frequencies, and represent a single, well-defined, relaxation process.

In summary, the local molecular structures of carbon allotropes have a strong effect on their dielectric spectra of up to 10^5 Hz. Given the static and featureless spectra for

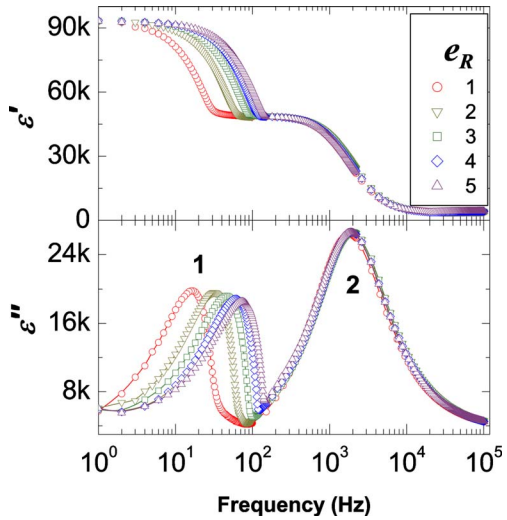

FIG. 2. (Color online) The electric field intensity dependence of $\varepsilon'(\omega)$ and $\varepsilon''(\omega)$ for the MWNT sample (in units of 1000). Upper panel legend lists the applied field factor e_R. For $\varepsilon''(\omega)$, the low-frequency mode is denoted by 1 and the high-frequency mode is denoted by 2.

TABLE I. Results of a linear fit to the mode-1 peak frequency f_1 as a function of electric field e_R. The slope m and intercept b (in the appropriate units) are given along with the regression coefficient R and the square-root of χ^2 per point. Note that all fits contain the same number of points ($N=5$) and so, the R and $\sqrt{(\chi^2/N)}$ can be quantitatively compared among each set.

Quantity	m (Hz)	b (Hz)	R	$\sqrt{(\chi^2/N)}$ (Hz)
f_1 (AG)	15.8 ± 0.1	0.8 ± 0.4	0.999 92	0.282
f_1 (MWNT)	14.2 ± 0.2	2.6 ± 0.7	0.999 63	0.548
f_1 (SWNT)	12.4 ± 0.6	3.6 ± 2.0	0.996 36	1.483

Downloaded 19 May 2008 to 130.215.36.230. Redistribution subject to AIP license or copyright; see http://apl.aip.org/apl/copyright.jsp

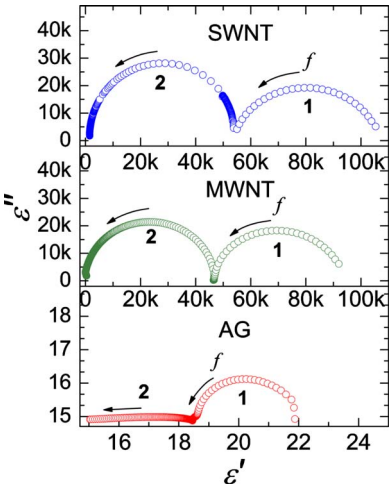

FIG. 4. (Color online) Cole–Cole plots of $\varepsilon''(\omega)$ vs $\varepsilon'(\omega)$ for the SWNT (top), MWNT (middle), and amorphous glass AG (bottom) carbon samples at e_R=2. Note that the upper two panels are in units of 1000. The arrows indicate the direction of increasing frequency and the labels denote the mode.

the diamond sample under identical experimental conditions, the two features in the spectra of the other carbon powders are intrinsic to their particular form and nature. For the glass, MWNT, and SWNT samples, the ac-electric field e_R plays an important role in linearly changing the peak position of mode 1 but does not affect the higher frequency mode 2. All samples are powders of comparable grain size but the diamond is an insulator while the glass is a conductor and the MWNT and SWNT are potential conductors depending on their chirality, which is not precisely known in our samples but highly likely. Thus, mode 1 is consistent with the buildup of space charges within the sample+cell, presumably at the grain/nanotube surfaces.

The mode 2 observed for the MWNT and SWNT appears as a single well-defined relaxation process, possibly due to orientational dynamics of permanent and/or induced dipoles in the graphene layers. The mode observed in the glass sample at similar frequencies is of a different character and likely related to the amorphous powder containing a range of distorted carbon structures, some of which are similar to nanotubes. The higher frequency of mode 2 in the MWNT compared to that in SWNT may be due to the "capacitorlike" structure of the multiple graphene walls and so, coupling of the polarization between layers. Coupling of polarization between the curved layers in MWNT would enhance dissipation and so, shifts this mode to higher frequencies. These results clearly indicate that the local structure plays a crucial role for mode 2 while mode 1 appears to be dictated by surfaces and the conducting nature of the samples. Additional experimental studies are planned but theoretical efforts are needed to fully understand the physics of these relaxation mechanisms.

[1] S. Iijima, Nature (London) **354**, 56 (1991).
[2] P. Poncharal, Z. L. Wang, D. Ugarate, and W. A. de Heer, Science **283**, 1513 (1999).
[3] J. W. Mintmire, B. I. Dunlap, and C. T. White, Appl. Phys. Lett. **68**, 631 (1992).
[4] L. Wang and Z.-M. Dang, Appl. Phys. Lett. **87**, 042903 (2005).
[5] Y. Xu, Y. Zhang, and E. Suhir, J. Appl. Phys. **100**, 074302 (2006).
[6] G. L. Zhao, D. Bagayoko, and L. Yang, J. Appl. Phys. **99**, 114311 (2006).
[7] S. Sinha, S. Barjami, G. Iannacchione, A. Schwab, and G. Muench, J. Nanopart. Res. **7**, 651 (2005).
[8] M. Han and L. Deng, Appl. Phys. Lett. **90**, 011101 (2007).
[9] X. Guo, D. Yu, Y. Gaol, Q. Li, W. Wan, and Z. Gao, *Proceedings of the 1st IEEE International Conference on Nano/Micro Engineered and Molecular Systems*, Zhuhai, China (IEEE, New York, 2006).
[10] O. Stephan, D. Taverna, M. Kociak, K. Suenaga, L. Henrard, and C. Colliex, Phys. Rev. B **66**, 155422 (2002).
[11] A. Madarhri, G. Pecastings, F. Carmona, and M. E. Achour, J. Microwave Optoelect. **6**, 36 (2007).
[12] Y. Sato, M. Terauchi, Y. Saito, and R. Saito, J. Electron Microsc. **55**, 137 (2006).
[13] K. Ahmad, W. Pan, and S.-L. Shi, Appl. Phys. Lett. **89**, 133122 (2006).
[14] P. Pötschke, S. M. Dudkin, and I. Alig, Polymer **44**, 5023 (2003).
[15] J. Leys, G. Sinha, C. Glorieux, and J. Thoen, Phys. Rev. E **71**, 051709 (2005).
[16] S. Pilla, J. A. Hamida, and N. S. Sullivan, Rev. Sci. Instrum. **70**, 4055 (1999).
[17] G. G. Raju, *Dielectrics in Electric Fields* (Dekker, New York, 2003).
[18] K. S. Cole and R. H. Cole, J. Chem. Phys. **9**, 341 (1941); **10**, 98 (1942).
[19] Y.-Z. Wei and S. Sridhar, J. Chem. Phys. **99**, 3119 (1993).
[20] D. W. Davidson and R. H. Cole, J. Chem. Phys. **19**, 1484 (1951).
[21] Y. Wei and S. Sridhar, J. Chem. Phys. **92**, 923 (1990).
[22] Y. Wei, P. Chiana, and S. Sridhar, J. Chem. Phys. **96**, 4569 (1992).
[23] *Relaxation Phenomena*, edited by W. Haase and S. Wrobel (Springer, Berlin, 2003).
[24] F. Kremer and A. Schonhals, *Broadband Dielectric Spectroscopy* (Springer, Berlin, 2003).

Downloaded 19 May 2008 to 130.215.36.230. Redistribution subject to AIP license or copyright; see http://apl.aip.org/apl/copyright.jsp